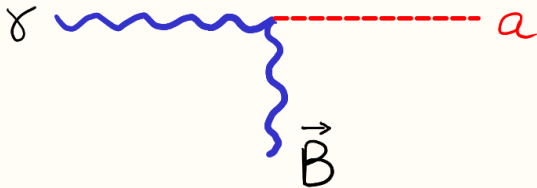


Constraints on Axions from Cosmic Distance Measurements

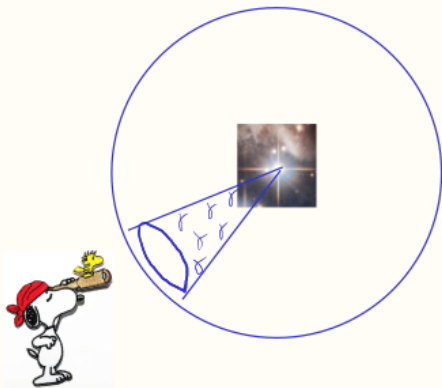
Manuel Buen-Abad, JiJi Fan, CS, 2011.05993

Basics of Axion-Photon Conversion

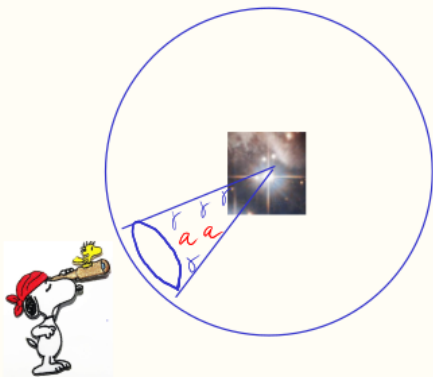


$$\mathcal{L}_{a\gamma} = -\frac{g_{a\gamma}}{4} a F_{\mu\nu} \tilde{F}^{\mu\nu} = g_{a\gamma} a \mathbf{E} \cdot \mathbf{B}$$

Basics of Axion-Photon Conversion

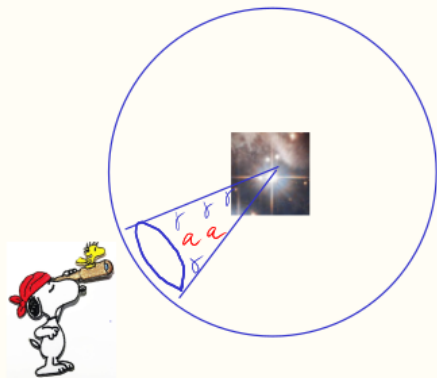


Basics of Axion-Photon Conversion



$$P \propto g_{a\gamma}^2 B^2 x^2$$

Basics of Axion-Photon Conversion

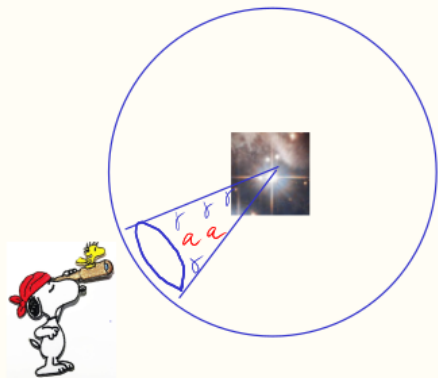


Main idea:

- Photon-axion **oscillation** directly affects the measured **brightness**.
- Modified **brightness** affects the inferred **distance**.

$$P \propto g_{a\gamma}^2 B^2 x^2$$

Basics of Axion-Photon Conversion



Main idea:

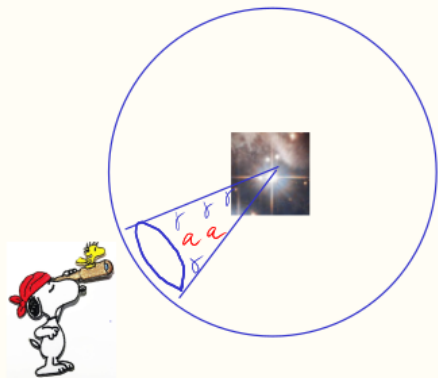
- Photon-axion **oscillation** directly affects the measured **brightness**.
- Modified **brightness** affects the inferred **distance**.

More specifically, it affects

- D_L : standard candle

$$P \propto g_{a\gamma}^2 B^2 x^2$$

Basics of Axion-Photon Conversion



$$P \propto g_{a\gamma}^2 B^2 x^2$$

Main idea:

- Photon-axion **oscillation** directly affects the measured **brightness**.
- Modified **brightness** affects the inferred **distance**.

More specifically, it affects

- D_L : standard candle
- D_A : (non-standard) rulers that rely on brightness to anchor its physical size

Type Ia Supernova

Type Ia supernova

$$F = \frac{L}{4\pi D_L^2},$$

Type Ia supernova

$$F = \frac{L}{4\pi D_L^2},$$

- Measure $F, D_L \Rightarrow L$ “anchor”

Type Ia supernova

$$F = \frac{L}{4\pi D_L^2},$$

- Measure $F, D_L \Rightarrow L$ “anchor”
- Measure $F \Rightarrow D_L$ “std candle”

Type Ia supernova

γ flux is conserved:

$$F = \frac{L}{4\pi D_L^2},$$

- Measure $F, D_L \Rightarrow L$ “anchor”
- Measure $F \Rightarrow D_L$ “std candle”

Type Ia supernova

γ flux is **not** converged:

$$F = \frac{L}{4\pi D_L^2},$$

Type Ia supernova

γ flux is **not** converged:

$$F = \frac{L}{4\pi D_L^2},$$

- Measure $F, D_L \Rightarrow L$ “anchor”

Type Ia supernova

γ flux is **not** converged:

$$F = P_{\gamma\gamma}(D_L) \frac{L}{4\pi D_L^2},$$

- Measure $F, D_L \Rightarrow L$ “anchor”
- Measure $F \Rightarrow P_{\gamma\gamma}(D_L)/D_L^2$

Type Ia supernova

γ flux is **not** converted:

$$F = P_{\gamma\gamma}(D_L) \frac{L}{4\pi D_L^2},$$

- Measure $F, D_L \Rightarrow L$ “anchor”
 - Measure $F \Rightarrow P_{\gamma\gamma}(D_L)/D_L^2$
-
- The $a - \gamma$ conversion modifies how we map flux F to the lum distance D_L

Type Ia supernova

γ flux is **not** converted:

$$F = P_{\gamma\gamma}(D_L) \frac{L}{4\pi D_L^2},$$

- Measure $F, D_L \Rightarrow L$ “anchor”
- Measure $F \Rightarrow P_{\gamma\gamma}(D_L)/D_L^2$

- The $a - \gamma$ conversion modifies how we map flux F to the lum distance D_L
- The shape of $F(D_L)$ is modified

Type Ia supernova

γ flux is **not** converted:

$$F = P_{\gamma\gamma}(D_L) \frac{L}{4\pi D_L^2},$$

- Measure $F, D_L \Rightarrow L$ “anchor”
- Measure $F \Rightarrow P_{\gamma\gamma}(D_L)/D_L^2$

- The $a - \gamma$ conversion modifies how we map flux F to the lum distance D_L
- The shape of $F(D_L)$ is modified
- In a Λ CDM universe, $D_L = D_L(z)$, this shows up as a change in $F(z)$ shape

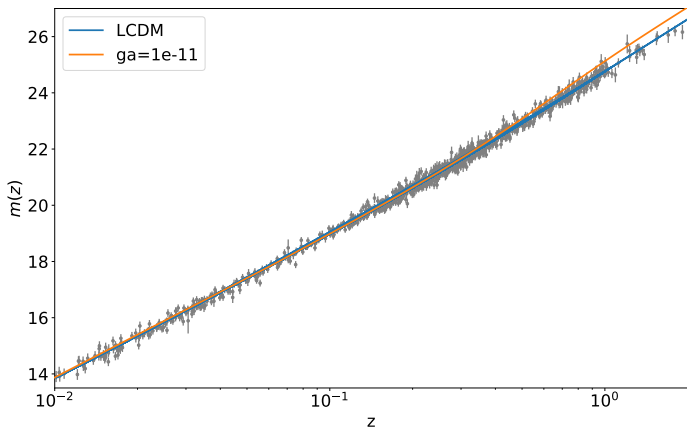
Type Ia supernova

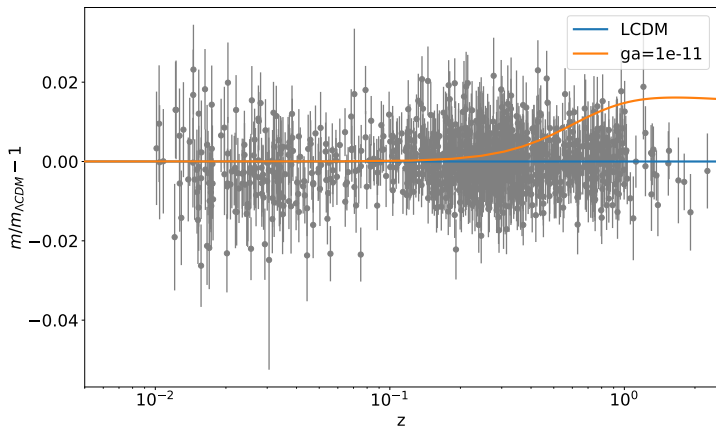
γ flux is **not** converted:

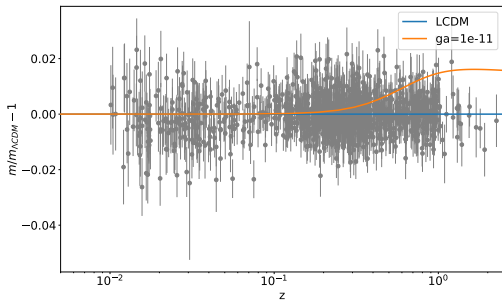
$$F = P_{\gamma\gamma}(D_L) \frac{L}{4\pi D_L^2},$$

- Measure $F, D_L \Rightarrow L$ “anchor”
- Measure $F \Rightarrow P_{\gamma\gamma}(D_L)/D_L^2$

- The $a - \gamma$ conversion modifies how we map flux F to the lum distance D_L
- The shape of $F(D_L)$ is modified
- In a Λ CDM universe, $D_L = D_L(z)$, this shows up as a change in $F(z)$ shape **which is constrained by SN Ia data set**







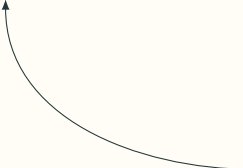
The likelihood:

$$-2 \ln \mathcal{L}_{Pan} = \sum_{i,j=1}^{1048} (m_i^{Pan} - m^{th}(z_i; \theta, M)) C_{ij}^{Pan} (m_j^{Pan} - m^{th}(z_j; \theta, M))$$

Galaxy Clusters

$$\theta \sim \frac{\ell}{D_A}$$

angular size


$$\theta \sim \frac{\ell}{D_A}$$

angular size

physical size

$$\theta \sim \frac{l}{D_A}$$

angular size

physical size

$$\theta \sim \frac{l}{D_A}$$

angular diameter distance

angular size

physical size

$$\theta \sim \frac{\ell}{D_A}$$

- $\gamma - a$ oscillation won't affect D_A if ℓ is known (std ruler)

angular diameter distance

angular size

$$\theta \sim \frac{\ell}{D_A}$$

- $\gamma - a$ oscillation won't affect D_A if ℓ is known (std ruler)
- Some objects have **unknown size** ℓ , which can only be inferred from their brightness measurement

angular diameter distance

Observable:

- X-ray surface brightness

$$S_X \propto \int n_e^2 \Lambda_{ee} d\ell = \int n_e^2 \Lambda_{ee} D_A d\theta$$

- Sunyaev-Zel'dovich Effect (SZE)

$$\Delta T_{CMB} \propto \int n_e T_e d\ell = \int n_e T_e D_A d\theta$$

$$D_A \propto \frac{\Delta T_{CMB}^2}{S_X}$$

$$D_A \propto \frac{\Delta T_{CMB}^2}{S_X}$$

With axions, the observables are affected as

$$\begin{aligned}\Delta T_{CMB} &\rightarrow \Delta T_{CMB} \times P_{\gamma\gamma}^{IGM}(\omega_{CMB}) \\ S_X &\rightarrow S_X \times P_{\gamma\gamma}^{IGM}(\omega_X) \langle P_{\gamma\gamma}^{ICM}(\omega_X) \rangle\end{aligned}$$

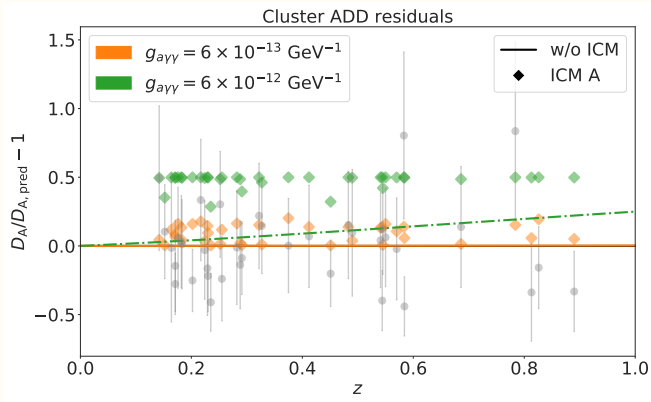
$$D_A \propto \frac{\Delta T_{CMB}^2}{S_X}$$

With axions, the observables are affected as

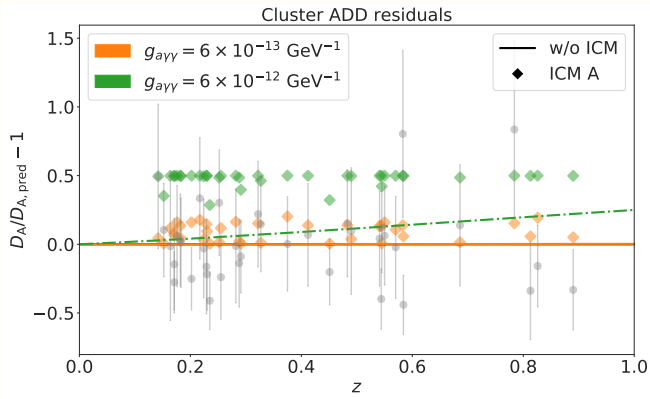
$$\begin{aligned}\Delta T_{CMB} &\rightarrow \Delta T_{CMB} \times P_{\gamma\gamma}^{IGM}(\omega_{CMB}) \\ S_X &\rightarrow S_X \times P_{\gamma\gamma}^{IGM}(\omega_X) \langle P_{\gamma\gamma}^{ICM}(\omega_X) \rangle\end{aligned}$$

which leads to a modification of the angular diameter distance

$$D_A \rightarrow D_A \times \frac{P_{\gamma\gamma}^{IGM}(\omega_{CMB})^2}{P_{\gamma\gamma}^{IGM}(\omega_X)} \langle P_{\gamma\gamma}^{ICM}(\omega_X) \rangle$$

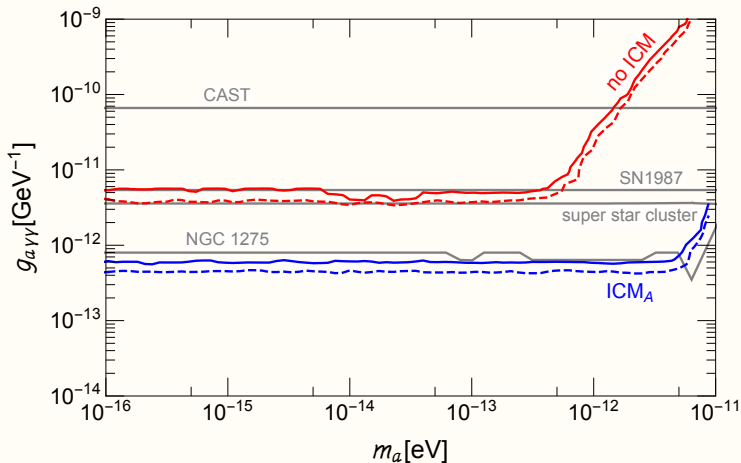


$$D_A \rightarrow D_A \times \frac{P_{\gamma\gamma}^{\text{IGM}}(\omega_{\text{CMB}})^2}{P_{\gamma\gamma}^{\text{IGM}}(\omega_X)} \langle P_{\gamma\gamma}^{\text{ICM}}(\omega_X) \rangle$$

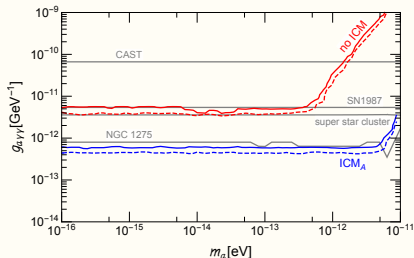


$$-2 \ln \mathcal{L}_{cl} = \sum_{i=1}^{38} \left(\frac{D_{A,i}^{exp} - D_A^{th}(z_i; \theta)}{\sigma_i^{exp}} \right)^2$$

Results – New Way to Constrain $a\gamma$ Coupling



Results – New Way to Constrain $a\gamma$ Coupling



- IGM

- ICM

- - with BAO (Planck r_s prior)

- with BAO (SH0ES M_0 prior)

 $B_{IGM} = 1 \text{ nG}$
 $B_{ICM} = 25 \mu\text{G} (n_e(r)/n_e(0))^{0.7}$
 $s_{IGM} = 1 \text{ Mpc}$
 $s_{ICM} \in (3.5 \text{ kpc}, 10 \text{ kpc})$

$$P(z)_{\gamma \rightarrow a}:$$

- IGM $\rightarrow D_L(z) \rightarrow$ SNIa data;
- ICM $\rightarrow D_A(z) \rightarrow$ clusters;
- Constraints on $m_a \lesssim 10^{-12} \text{ eV}$
- Independent of H_0 tension
- Different systematics from other bounds (*i.e.* CMB spectrum)
 - IGM: $g_{a\gamma\gamma} \propto B_{IGM}^{-1} s_{IGM}^{-1/2}$
 - ICM: quantified w/ B_{ICM} models
- Improvements:
 - $F(z)$ SNe
 - S_X and ΔT_{CMB} in galaxy clusters
 - B_{IGM}, B_{ICM}

Back up slides

Photon-axion oscillation

In a homogeneous environment:

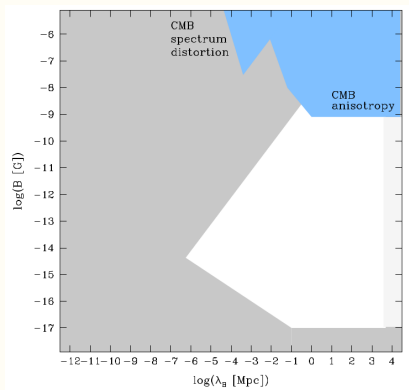
$$P_{\gamma \rightarrow a} = \frac{(2\Delta)^2}{k^2} \sin^2 \left(\frac{kx}{2} \right) \\ = \frac{g_{a\gamma}^2 B^2}{g_{a\gamma}^2 B^2 + (m_a^2 - m_\gamma^2)^2 / (4\omega^2)} \sin^2 \left(\left(\frac{1}{2} \sqrt{g_{a\gamma}^2 B^2 + \frac{(m_a^2 - m_\gamma^2)^2}{4\omega^2}} \right) x \right),$$

where m_γ is the photon plasma frequency, $m_\gamma^2 = \frac{4\pi\alpha n_e}{m_e}$.

Three scales: Δ, k, x .

	$kx < 1$	$kx > 1$
$\Delta \sim k$	$\frac{1}{4} g_{a\gamma}^2 B^2 x^2$	$\sim \frac{1}{2}$
$\Delta \ll k$	$\frac{1}{4} g_{a\gamma}^2 B^2 x^2$	$\frac{2g_{a\gamma}^2 B^2}{(m_a^2 - m_\gamma^2)/\omega^2}$

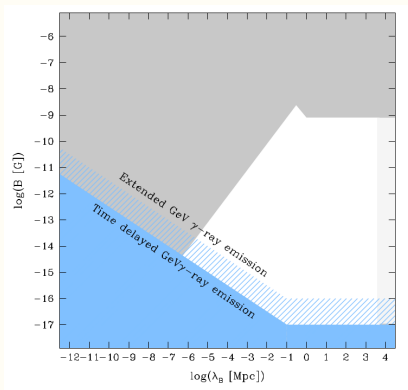
IGM – magnetic field strength



IGM magnetic field:

- CMB anisotropies, lack of Faraday rotation of quasars, $B_{IGM} \lesssim \text{nG}$.

IGM – magnetic field strength



IGM magnetic field:

- CMB anisotropies, lack of Faraday rotation of quasars, $B_{IGM} \lesssim \text{nG}$.
- Non-observation of cascade emission of TeV γ -ray, $B_{IGM} \gtrsim 10^{-16} \text{ G}$.

IGM – magnetic field strength

Note that in the oscillation formula,

$$P_0 = \frac{g_{a\gamma}^2 B^2}{g_{a\gamma}^2 B^2 + (m_a^2 - m_\gamma^2)^2 / (4\omega^2)} \sin^2 \left(\left(\frac{1}{2} \sqrt{g_{a\gamma}^2 B^2 + \frac{(m_a^2 - m_\gamma^2)^2}{4\omega^2}} \right) z \right),$$

$(g_{a\gamma} B)$ shows up hand-in-hand.

- So what we bound in IGM is actually on $(g_{a\gamma} B)$.
- In this work, we take common benchmark $B_{IGM} \sim \text{nG}$.
- Future detection of $B_{IGM} < \text{nG}$ will rescale the bounds on $g_{a\gamma}$ as B_{IGM}/nG .

c.f. Durrer and Neronov 2013, Vachaspati 2010

$$P_0 = \frac{g_{a\gamma}^2 B^2}{g_{a\gamma}^2 B^2 + (m_a^2 - m_\gamma^2)^2 / (4\omega^2)} \sin^2 \left(\left(\frac{1}{2} \sqrt{g_{a\gamma}^2 B^2 + \frac{(m_a^2 - m_\gamma^2)^2}{4\omega^2}} \right) z \right),$$

At low redshift, $z < 0.5$,

$$\text{baryons} \begin{cases} \text{Lyman-}\alpha \text{ forest, } 28 \pm 11\%, \gtrsim 90\% \text{ volume} \\ \text{warm-hot intergalactic matter, } \lesssim 10\% \text{ volume} \end{cases}$$

- $\bar{n}_{e, Ly\alpha} \approx 6.5 \times 10^{-8} \text{ cm}^{-3}$

IGM – electron density

At low redshift, $z < 0.5$,

$$\text{baryons} \begin{cases} \text{Lyman-}\alpha \text{ forest, } 28 \pm 11\%, \gtrsim 90\% \text{ volume} \\ \text{warm-hot intergalactic matter, } \lesssim 10\% \text{ volume} \end{cases}$$

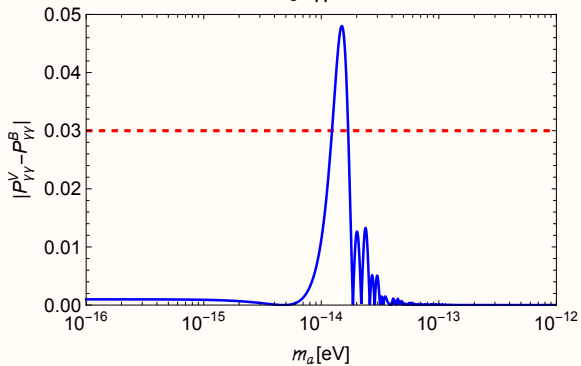
- $\bar{n}_{e, Ly\alpha} \approx 6.5 \times 10^{-8} \text{ cm}^{-3}$

Simulation shows at $z < 1$ *(c.f. Martizzi 2018)*

$$\text{Lyman-}\alpha \begin{cases} \text{underdense patches, a.k.a. cosmic voids} & \sim 30 - 50\% \text{ vol.} \\ \text{2D structures, a.k.a. sheets} & \sim 30 - 50\% \text{ vol.} \end{cases}$$

- $n_e \approx 1.6 \times 10^{-8} \text{ cm}^{-3}$ (cosmic voids)
- $n_e \approx 3.0 \times 10^{-8} \text{ cm}^{-3}$ (sheets)

$N=3000, g_{a\gamma\gamma}=10^{-11}\text{ GeV}$



The ICM electron density can be modeled using the double- β profile

$$n_{e,ICM} = n_{e,0} \left(f \left(1 + \frac{r^2}{r_{c1}^2} \right)^{-\frac{3\beta}{2}} + (1 - f) \left(1 + \frac{r^2}{r_{c2}^2} \right)^{-\frac{3\beta}{2}} \right)$$

- “Regular” clusters (Coma-like): single beta $f = 1$
- “Cool-core” clusters (Perseus-like): double- β to account for the core

Cluster	N (10^{-25} g cm $^{-3}$)	r_s (arcsec)	n_{e0} (cm $^{-3}$)	r_{c1} (arcsec)	β	f	r_{c2} (arcsec)	D_A Gpc
CL 0016+1609	0.10 $^{+0.14}_{-0.06}$	225 $^{+233}_{-96}$	1.40 $^{+0.18}_{-0.15}$ $\times 10^{-2}$	10.3 $^{+4.4}_{-2.5}$	0.761 $^{+0.031}_{-0.036}$	0.48 $^{+0.05}_{-0.05}$	47.8 $^{+3.8}_{-3.7}$	1.38 $^{+0.22}_{-0.22}$
Abell 0068	3.29 $^{+7.60}_{-2.51}$	70 $^{+62}_{-27}$	8.89 $^{+1.68}_{-1.78}$ $\times 10^{-3}$	–	0.693 $^{+0.026}_{-0.028}$	–	47.8 $^{+2.8}_{-3.0}$	0.63 $^{+0.16}_{-0.16}$
Abell 0267	2.02 $^{+3.04}_{-1.24}$	75 $^{+50}_{-31}$	1.17 $^{+0.11}_{-0.10}$ $\times 10^{-2}$	–	0.698 $^{+0.031}_{-0.030}$	–	40.9 $^{+2.8}_{-2.8}$	0.60 $^{+0.11}_{-0.09}$
Abell 0370	1.63 $^{+1.80}_{-0.57}$	51 $^{+13}_{-21}$	5.33 $^{+0.58}_{-0.40}$ $\times 10^{-3}$	–	0.740 $^{+0.035}_{-0.028}$	–	55.6 $^{+3.1}_{-2.6}$	1.08 $^{+0.19}_{-0.20}$
MS 0451.6-0305	0.27 $^{+0.16}_{-0.17}$	110 $^{+74}_{-102}$	1.26 $^{+0.09}_{-0.09}$ $\times 10^{-2}$	–	0.777 $^{+0.019}_{-0.019}$	–	34.5 $^{+1.1}_{-1.1}$	1.42 $^{+0.26}_{-0.26}$
MACS J0647.7+7015	12.01 $^{+16.07}_{-8.11}$	36 $^{+22}_{-13}$	2.19 $^{+0.34}_{-0.25}$ $\times 10^{-2}$	–	0.653 $^{+0.019}_{-0.017}$	–	19.9 $^{+1.2}_{-1.2}$	0.77 $^{+0.21}_{-0.18}$
Abell 0586	1.78 $^{+1.97}_{-1.05}$	102 $^{+40}_{-26}$	1.83 $^{+0.25}_{-0.21}$ $\times 10^{-2}$	–	0.627 $^{+0.017}_{-0.013}$	–	32.0 $^{+1.7}_{-1.4}$	0.52 $^{+0.15}_{-0.12}$
MACS J0744.8+3927	0.27 $^{+0.22}_{-0.22}$	94 $^{+102}_{-51}$	1.14 $^{+0.15}_{-0.15}$ $\times 10^{-1}$	3.4 $^{+0.6}_{-0.7}$	0.635 $^{+0.049}_{-0.039}$	0.93 $^{+0.01}_{-0.01}$	25.8 $^{+1.7}_{-1.7}$	1.68 $^{+0.38}_{-0.38}$
Abell 0611	1.73 $^{+1.87}_{-0.60}$	64 $^{+15}_{-12}$	5.27 $^{+0.97}_{-1.00}$ $\times 10^{-2}$	2.8 $^{+0.4}_{-0.3}$	0.600 $^{+0.014}_{-0.008}$	0.66 $^{+0.08}_{-0.07}$	22.5 $^{+1.6}_{-1.2}$	0.78 $^{+0.18}_{-0.18}$
Abell 0665	0.18 $^{+0.14}_{-0.03}$	340 $^{+150}_{-163}$	9.13 $^{+1.34}_{-0.99}$ $\times 10^{-3}$	3.2 $^{+0.8}_{-0.5}$	0.730 $^{+0.015}_{-0.016}$	0.11 $^{+0.10}_{-0.08}$	64.4 $^{+1.7}_{-1.6}$	0.66 $^{+0.09}_{-0.10}$
Abell 0697	0.76 $^{+0.59}_{-1.38}$	93 $^{+66}_{-32}$	9.82 $^{+1.09}_{-1.28}$ $\times 10^{-3}$	–	0.584 $^{+0.016}_{-0.020}$	–	41.6 $^{+1.6}_{-1.9}$	0.88 $^{+0.30}_{-0.23}$
Abell 0773	1.22 $^{+1.38}_{-0.88}$	54 $^{+40}_{-19}$	8.04 $^{+0.68}_{-0.64}$ $\times 10^{-3}$	–	0.564 $^{+0.022}_{-0.022}$	–	40.2 $^{+2.2}_{-2.3}$	0.98 $^{+0.17}_{-0.14}$
ZW 3146	0.66 $^{+0.08}_{-0.05}$	121 $^{+4}_{-4}$	1.70 $^{+0.02}_{-0.02}$ $\times 10^{-1}$	4.4 $^{+0.1}_{-0.1}$	0.668 $^{+0.005}_{-0.004}$	0.881 $^{+0.004}_{-0.003}$	25.5 $^{+0.7}_{-0.4}$	0.83 $^{+0.02}_{-0.02}$
MS 1054-0321	0.04 $^{+0.08}_{-0.02}$	666 $^{+571}_{-359}$	6.15 $^{+0.71}_{-0.56}$ $\times 10^{-3}$	–	1.791 $^{+0.148}_{-0.209}$	–	83.7 $^{+4.9}_{-7.3}$	1.33 $^{+0.28}_{-0.26}$
MS 1137.5+6625	1.73 $^{+1.40}_{-0.40}$	16 $^{+9}_{-8}$	1.26 $^{+0.11}_{-0.11}$ $\times 10^{-2}$	–	0.667 $^{+0.044}_{-0.043}$	–	14.2 $^{+3.3}_{-3.3}$	2.85 $^{+0.63}_{-0.63}$
MACS J1149.5+2223	0.74 $^{+0.50}_{-0.50}$	110 $^{+49}_{-51}$	8.53 $^{+0.89}_{-0.85}$ $\times 10^{-3}$	–	0.673 $^{+0.022}_{-0.022}$	–	42.8 $^{+2.4}_{-2.4}$	0.80 $^{+0.16}_{-0.16}$
Abell 1413	0.47 $^{+0.58}_{-0.47}$	121 $^{+51}_{-47}$	3.66 $^{+0.65}_{-0.49}$ $\times 10^{-2}$	6.5 $^{+1.5}_{-1.3}$	0.531 $^{+0.018}_{-0.014}$	0.76 $^{+0.02}_{-0.02}$	39.3 $^{+4.5}_{-4.5}$	0.78 $^{+0.18}_{-0.18}$
CL J1226.9+3332	4.09 $^{+9.41}_{-3.58}$	46 $^{+58}_{-19}$	3.01 $^{+0.49}_{-0.44}$ $\times 10^{-2}$	–	0.715 $^{+0.034}_{-0.038}$	–	15.8 $^{+1.3}_{-1.3}$	1.08 $^{+0.42}_{-0.28}$
MACS J1311.0-0310	7.59 $^{+17.81}_{-7.09}$	19 $^{+9}_{-9}$	3.93 $^{+0.22}_{-0.55}$ $\times 10^{-2}$	–	0.613 $^{+0.022}_{-0.020}$	–	9.3 $^{+0.7}_{-0.7}$	1.38 $^{+0.37}_{-0.37}$
Abell 1689	2.68 $^{+1.20}_{-1.16}$	75 $^{+19}_{-19}$	4.054 $^{+0.36}_{-0.26}$ $\times 10^{-2}$	21.7 $^{+0.9}_{-0.9}$	0.873 $^{+0.039}_{-0.041}$	0.87 $^{+0.01}_{-0.01}$	104.9 $^{+5.1}_{-5.5}$	0.65 $^{+0.09}_{-0.09}$
RX J1347.5-1145	4.57 $^{+1.06}_{-0.86}$	47 $^{+5}_{-5}$	2.81 $^{+0.16}_{-0.15}$ $\times 10^{-1}$	3.9 $^{+0.2}_{-0.2}$	0.631 $^{+0.009}_{-0.008}$	0.942 $^{+0.004}_{-0.003}$	22.9 $^{+1.8}_{-1.4}$	0.96 $^{+0.06}_{-0.06}$
MS 1358.4+6245	0.58 $^{+0.19}_{-0.19}$	90 $^{+26}_{-18}$	9.62 $^{+0.78}_{-0.78}$ $\times 10^{-2}$	3.3 $^{+0.2}_{-0.2}$	0.675 $^{+0.016}_{-0.013}$	0.934 $^{+0.003}_{-0.003}$	37.2 $^{+1.9}_{-1.9}$	1.13 $^{+0.30}_{-0.30}$
Abell 1835	1.18 $^{+0.03}_{-0.03}$	150 $^{+11}_{-11}$	1.10 $^{+0.02}_{-0.02}$ $\times 10^{-1}$	9.3 $^{+0.2}_{-0.2}$	0.798 $^{+0.017}_{-0.017}$	0.991 $^{+0.001}_{-0.001}$	63.7 $^{+1.6}_{-1.6}$	1.07 $^{+0.10}_{-0.10}$
MACS J1423.8+2504	1.83 $^{+0.02}_{-0.07}$	33 $^{+1}_{-1}$	1.60 $^{+0.02}_{-0.08}$ $\times 10^{-1}$	4.2 $^{+0.1}_{-0.1}$	0.721 $^{+0.012}_{-0.008}$	0.975 $^{+0.001}_{-0.001}$	36.7 $^{+0.9}_{-0.9}$	1.49 $^{+0.08}_{-0.08}$
Abell 1914	5.79 $^{+2.60}_{-1.85}$	81 $^{+14}_{-11}$	1.72 $^{+0.13}_{-0.08}$ $\times 10^{-2}$	6.6 $^{+0.6}_{-0.6}$	0.899 $^{+0.007}_{-0.012}$	0.008 $^{+0.018}_{-0.008}$	68.3 $^{+0.7}_{-1.0}$	0.44 $^{+0.04}_{-0.05}$
Abell 1995	0.07 $^{+0.06}_{-0.04}$	359 $^{+205}_{-117}$	9.35 $^{+0.74}_{-0.56}$ $\times 10^{-3}$	31.2 $^{+3.0}_{-3.5}$	1.298 $^{+0.062}_{-0.096}$	0.462 $^{+0.033}_{-0.033}$	83.5 $^{+5.7}_{-7.1}$	1.19 $^{+0.15}_{-0.14}$
Abell 2111	0.47 $^{+2.74}_{-0.38}$	172 $^{+354}_{-107}$	5.99 $^{+1.05}_{-0.99}$ $\times 10^{-3}$	–	0.600 $^{+0.024}_{-0.025}$	–	50.4 $^{+3.8}_{-3.8}$	0.64 $^{+0.20}_{-0.17}$
Abell 2163	0.26 $^{+0.12}_{-0.12}$	390 $^{+87}_{-87}$	1.09 $^{+0.07}_{-0.07}$ $\times 10^{-2}$	4.0 $^{+1.3}_{-1.3}$	0.560 $^{+0.004}_{-0.004}$	0.022 $^{+0.037}_{-0.022}$	66.8 $^{+0.9}_{-0.9}$	0.52 $^{+0.04}_{-0.04}$
Abell 2204	0.92 $^{+0.30}_{-0.15}$	120 $^{+13}_{-18}$	2.01 $^{+0.12}_{-0.09}$ $\times 10^{-1}$	7.5 $^{+0.3}_{-0.3}$	0.710 $^{+0.031}_{-0.025}$	0.960 $^{+0.003}_{-0.004}$	67.4 $^{+1.8}_{-1.8}$	0.61 $^{+0.06}_{-0.06}$
Abell 2218	1.02 $^{+0.59}_{-0.60}$	110 $^{+22}_{-22}$	7.02 $^{+0.66}_{-0.66}$ $\times 10^{-3}$	–	0.739 $^{+0.017}_{-0.017}$	–	63.3 $^{+1.4}_{-2.1}$	0.66 $^{+0.11}_{-0.11}$
RX J1716.4+6708	0.34 $^{+3.38}_{-0.39}$	146 $^{+545}_{-49}$	1.94 $^{+0.61}_{-0.40}$ $\times 10^{-2}$	–	0.589 $^{+0.042}_{-0.035}$	–	12.8 $^{+2.0}_{-2.0}$	1.04 $^{+0.53}_{-0.53}$
Abell 2259	0.65 $^{+0.54}_{-0.54}$	141 $^{+155}_{-25}$	9.29 $^{+2.97}_{-1.71}$ $\times 10^{-3}$	–	0.560 $^{+0.025}_{-0.024}$	–	41.0 $^{+3.9}_{-2.5}$	0.58 $^{+0.29}_{-0.25}$
Abell 2261	1.36 $^{+0.85}_{-1.41}$	68 $^{+25}_{-17}$	4.16 $^{+0.53}_{-0.63}$ $\times 10^{-2}$	10.0 $^{+1.9}_{-1.7}$	0.628 $^{+0.025}_{-0.022}$	0.77 $^{+0.04}_{-0.05}$	37.8 $^{+2.5}_{-2.5}$	0.73 $^{+0.20}_{-0.13}$
MS 2053.7-0449	0.26 $^{+0.22}_{-0.22}$	40 $^{+22}_{-22}$	9.22 $^{+0.92}_{-0.92}$ $\times 10^{-3}$	–	0.522 $^{+0.042}_{-0.042}$	–	10.8 $^{+1.9}_{-1.7}$	2.48 $^{+0.44}_{-0.44}$

We follow previous studies and assume a B_{ICM} profile

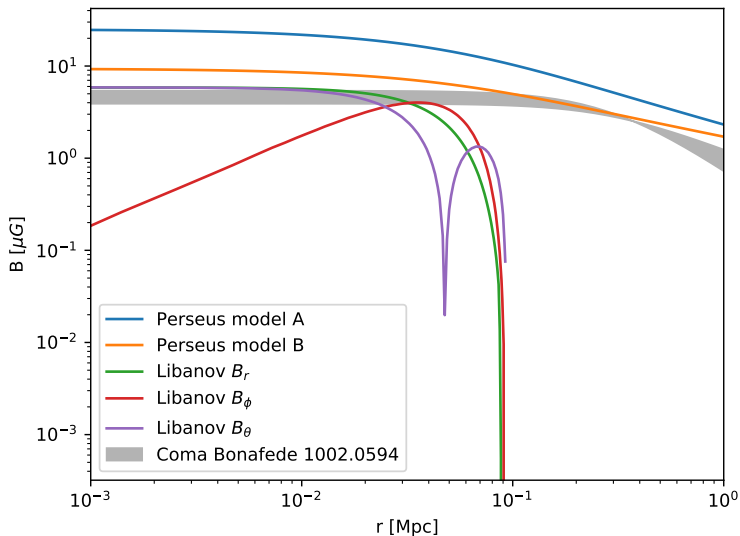
$$B_{ICM} = B_{ref} \left(\frac{n_e(r)}{n_e(r_{ref})} \right)^\eta$$

with two profiles similar to Perseus, and one similar to Coma

Model	r_{ref}	B_{ref}	η
A	0 kpc	25 μ G	0.7
B	25 kpc	7.5 μ G	0.5
C	0 kpc	4.7 μ G	0.5

*Bonafede et al. 2010, Feretti et al. 2012,
Reynolds et al. 2019, Angus et al. 2014*

ICM – Magnetic field



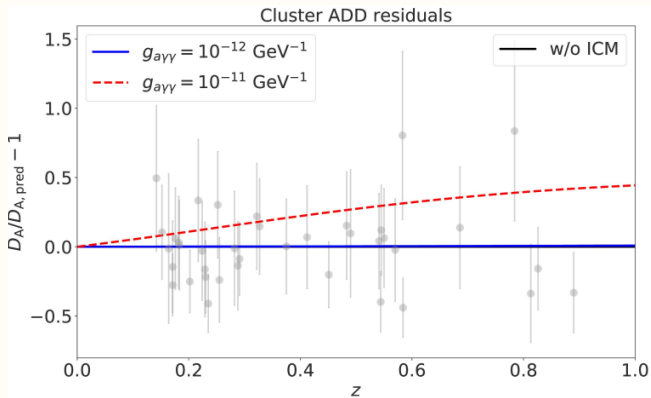
We follow previous studies and assume a B_{ICM} profile

$$B_{ICM} = B_{ref} \left(\frac{n_e(r)}{n_e(r_{ref})} \right)^\eta$$

with two profiles similar to Perseus, and one similar to Coma

Model	r_{ref}	B_{ref}	η
A	0 kpc	25 μ G	0.7
B	25 kpc	7.5 μ G	0.5
C	0 kpc	4.7 μ G	0.5
no ICM	n/a	0 μ G	n/a

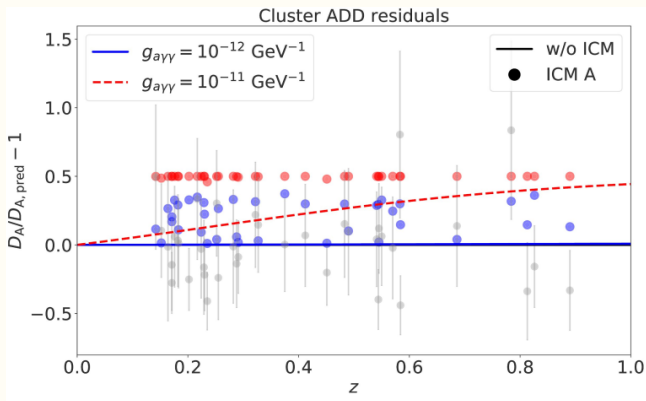
*Bonafede et al. 2010, Feretti et al. 2012,
Reynolds et al. 2019, Angus et al. 2014,
Libanov and Troitsky 2020*



$$\Delta T_{CMB} \rightarrow \Delta T_{CMB} \times P_{\gamma\gamma}^{IGM}(\omega_{CMB})$$

$$S_X \rightarrow S_X \times P_{\gamma\gamma}^{IGM}(\omega_X)$$

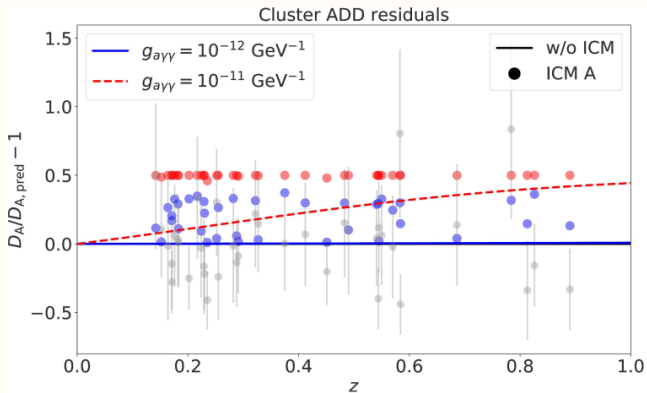
$$D_A \rightarrow D_A \times \frac{P_{\gamma\gamma}^{IGM}(\omega_{CMB})^2}{P_{\gamma\gamma}^{IGM}(\omega_X)}$$



$$\Delta T_{CMB} \rightarrow \Delta T_{CMB} \times P_{\gamma\gamma}^{IGM}(\omega_{CMB})$$

$$S_X \rightarrow S_X \times P_{\gamma\gamma}^{IGM}(\omega_X) \langle P_{\gamma\gamma}^{ICM}(\omega_X) \rangle$$

$$D_A \rightarrow D_A \times \frac{P_{\gamma\gamma}^{IGM}(\omega_{CMB})^2}{P_{\gamma\gamma}^{IGM}(\omega_X)} \langle P_{\gamma\gamma}^{ICM}(\omega_X) \rangle$$



$$-2 \ln \mathcal{L}_{cl} = \sum_{i=1}^{38} \left(\frac{D_{A,i}^{exp} - D_A^{th}(z_i; \theta)}{\sigma_i^{exp}} \right)^2$$

Other data sets

- SH0ES:

$$-2 \ln \mathcal{L}_{SH0ES} = \sum_{i=1}^{19} \left(\frac{m_{10,i}^{SH0ES} - m_{10}}{\sigma_i^{SH0ES}} \right)^2$$

- TDCOSMO:

$$-2 \ln \mathcal{L}_{TDCOSMO} = \left(\frac{H_0^{TD} - H_0}{\sigma^{TD}} \right)^2$$

- BAO: (BOSS DR12 CMASS and LOWZ; 6dFGS, MGS)

$$-2 \ln \mathcal{L}_{BAO} = \sum_{i,j} \Delta_i C_{ij}^{BAO} \Delta_j$$

$$\Delta_i = (Q_i^{BAO} - Q^{\Lambda CDM}(z_i; \Omega_\Lambda, H_0, r_s^{drag}))$$

- Planck

$$-2 \ln \mathcal{L}_{Pl} = \left(\frac{r_s^{Pl} - r_s}{\sigma^{Pl}} \right)^2$$

Late vs Early

- The theory parameters:

$$\theta = \left(\underbrace{H_0, \Omega_\Lambda}_{\Lambda\text{CDM}}; \underbrace{m_a, g_{a\gamma}}_{\text{axion}}; \underbrace{m_{10}, r_s^{\text{drag}}}_{\text{nuisance}} \right)$$

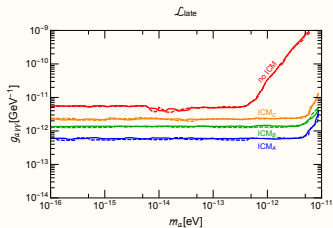
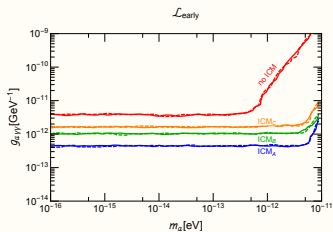
- The likelihoods:

$$\mathcal{L}_{\text{early}} \equiv \mathcal{L}_{\text{Pan}} \cdot \mathcal{L}_{\text{cluster}} \cdot \mathcal{L}_{\text{BAO}} \cdot \mathcal{L}_{\text{PI}}$$

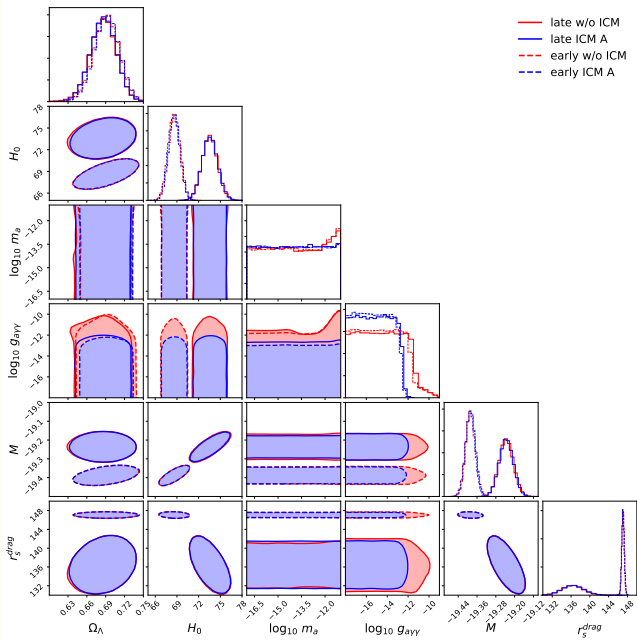
$$\mathcal{L}_{\text{late}} = \mathcal{L}_{\text{Pan}} \cdot \mathcal{L}_{\text{cluster}} \cdot \mathcal{L}_{\text{BAO}} \cdot \mathcal{L}_{\text{SH0ES}} \cdot \mathcal{L}_{\text{TD}}$$

- Production runs:

$$\left\{ \begin{array}{l} \text{early} \\ \text{late} \end{array} \right\} \otimes \left\{ \begin{array}{l} n_e^{\text{IGM}} = 1.6 \times 10^{-8} \text{ cm}^{-3} \\ n_e^{\text{IGM}} = 3.0 \times 10^{-8} \text{ cm}^{-3} \end{array} \right\} \otimes \left\{ \begin{array}{l} \text{ICM A} \\ \text{ICM B} \\ \text{ICM C} \\ \text{no ICM} \end{array} \right\}$$



- Little difference between $n_e^{IGM} = 1.6 \times 10^{-8}$ and $3.0 \times 10^{-8} \text{ cm}^{-3}$
 - linear to nonlinear regime triggered by m_a
- Small difference between early and late
 - What matters most is the shape of $H(z)$
- “ICM A” is most optimistic, “no ICM” most conservative.
 - Only in ‘no ICM’ runs the constraint is on $g_{a\gamma} B$



Interface:

- `cosmo_axions_run.py`
- `cosmo_axions_analysis.py`

Interface:

- `cosmo_axions_run.py` `$python cosmo_axions_run.py -L likelihoods/ -o path/to/output/ -i inputs/the_param_file.param -N chain_length -w number_of_walkers`
- `cosmo_axions_analysis.py` `$python cosmo_axions_analysis.py -i path/to/your/chain/`

Interface:

- `cosmo_axions_run.py`
- `cosmo_axions_analysis.py`

Internal:

- `data.py`
- `chi2.py`
- `cosmo.py`
- `ag_probs.py`
- `icm.py`
- `igm.py`

Interface:

- `cosmo_axions_run.py`
- `cosmo_axions_analysis.py`

Internal:

- `data.py` data loading and initialization
- `chi2.py` defines $\log(|k|)$ of each data set
- `cosmo.py` cosmological functions, $H(z)$, $D_A(z)$, $\tau(z)$, etc.
- `ag_probs.py` axion-photon related functions, $m_\gamma(n_e)$, $P(z)$, etc.
- `icm.py` ICM related functions, $n_e^{ICM}(r)$, $P_{ICM}(r)$, etc.
- `igm.py` IGM related functions, $P_{IGM}(r)$, etc.

likelihoods/

- BAO
- cluster
- Pantheon
- SH0ES

likelihoods/

- BAO BAO_*.txt
- cluster add.txt, bonamente_add.txt
- Pantheon lcpam*.txt, sys_*.txt
- SH0ES lstAnchor.csv

inputs/

- likelihoods to use:

```
...
use_TDCOSMO = True
use_SHOES = True
use_early = False
use_Pantheon = True
use_BOSSDR12 = True
use_BAOlowz = True
use_clusters = True
...
```

- range to scan:

```
# var = [initial, low, up, step]
OmL = [0.6847, 0.6, 0.75, 0.015]
h0 = [ 0.73, 0.6, 0.8, 0.02]
logma = [ -14, -17, -11, 0.25]
logga = [ -11, -18., -8., 0.1]
M0 = [ -19.3, -21, -18, 0.1]
rs = [147.78, 120., 160., 1.]
```


inputs/

- likelihoods to use:

```
...
use_TDCOSMO = True
use_SHOES = True
use_early = False
use_Pantheon = True
use_BOSSDR12 = True
use_BAOlowz = True
use_clusters = True
...
```

- range to scan:

```
# var = [initial, low, up, step]
OmL = [0.6847, 0.6, 0.75, 0.015]
h0 = [ 0.73, 0.6, 0.8, 0.02]
logma = [ -14, -17, -11, 0.25]
logga = [ -11, -18., -8., 0.1]
M0 = [ -19.3, -21, -18, 0.1]
rs = [147.78, 120., 160., 1.]
```

Pull requests, forks, and
issue tickets are all
welcomed!